Int J Clin Exp Pathol 2025;18(6):245-257
www.ijcep.com /ISSN:1936-2625/IJCEP0164499

Original Article

Grossly visible non-invasive neoplasm of the gallbladder: method of classification and its relationship to pyloric gland adenoma

Miyu Ichida, Yuki Fukumura, Takashi Yao

Department of Human Pathology, School of Medicine, Juntendo University, Tokyo 113-0033, Japan

Received March 12, 2025; Accepted May 10, 2025; Epub June 15, 2025; Published June 30, 2025

Abstract: Objectives: To devise a classification method for grossly visible non-invasive neoplasms (GVNINs) of the gallbladder and examine their relationship to pyloric gland adenoma (PGA), since clinicopathological features of GVNINs are not well known to date and the relationship between PGA and GVNINs remains unknown. Methods: Eighty-five GVNINs were classified into pedunculated (PE), sessile type 1 (SE1), and sessile type 2 (SE2) groups, and into histologic subtypes. Clinicopathologic data, immunohistochemical data surrogating gene abnormalities, and mutational data of CTNNB1, KRAS, and GNAS were obtained. In five cases of SE1 containing PGA-like lesions, separate analyses for PGA-like and non-PGA-like lesions were performed. The relevance of the mucinous tumor cell ratio was analyzed in PE tumors. Results: The invasion rates were 0%, 33.4%, and 91.2% for PE, SE1, and SE2, respectively. SE2 was more with ≥ pT2 (78.2%) compared to SE1 (16.7%). All PE and SE1 were of gastric pyloric subtype and gastric type, respectively, whereas pancreatobiliary/intestinal subtypes were predominant in SE2. Approximately 66.7% of SE1 had β-catenin abnormalities, STK11-loss, and CTNNB1 mutation. SMAD4-loss was exclusively seen in the intestinal subtype. Mucinous cell-predominant PGA was not clinicopathologically different from non-mucinous cell-dominant type except for patients' age and nuclear β-catenin labeling index. PGA and PGA-like lesions in SE1 shared β-catenin abnormalities and CTNNB1 mutation, but not STK11-loss. Conclusions: A clinicopathologically relevant classification system for GVNINs was proposed. Histologic subtyping was also important. Non-mucinous cell-predominant PE was suggested to be a similar entity to PGA, while SE1 containing PGA-like lesions were not suggested to be similar.

Keywords: Gallbladder, non-invasive neoplasm, intracholecystic papillary neoplasm, pyloric gland adenoma, β-catenin, STK11

Introduction

Precancerous lesions of the gallbladder are classified into flat (including low or micropapillary) and elevated (grossly visible non-invasive neoplasm, GVNIN) types. The flat type is microscopically defined as flat or micropapillary and has been named "biliary intraepithelial neoplasia (BilIN)" [1]. Compared to other GVNINs of the pancreatobiliary system, such as intraductal papillary mucinous neoplasms (IPMNs) and intraductal tubulopapillary neoplasms (ITPNs) of the pancreas and intraductal papillary neoplasms of the bile ducts (IPNBs), GVNINs of the gallbladder have not been well-characterized [2]. Regarding GVNIN, many terminologies for several groups of tumors have been proposed, such as intracholecystic papillary neoplasm (ICPN), pyloric gland adenoma (PGA), papillary carcinoma, and intracholecystic tubular non-mucinous neoplasm (ICTN) [3-6]. ICPN is macroscopically characterized by broad-based, exophytic tumors, and grows in a predominant papillary configuration for the typical histopathology. Conversely, the typical histopathology of PGA is composed of uniform back-to-back mucinous glands in a tubular configuration [1]. The GVNINs composed of small non-mucinous tubules with complex architecture were proposed to be ICTN [5, 6] and those mainly consisting of papillary or papillotubular adenocarcinomas with an overall complex architecture (more complex than that expected in typical IPNBs) were categorized as papillary carcinoma by several researchers [3, 4]. However, the definition or separation of these tumor groups has

https://doi.org/10.62347/WLEU6787

not yet been standardized, and different researchers still use different classification systems for these GVNINs. Recent comprehensive molecular studies have clarified several oncogenic molecular alterations that are detectable in gallbladder carcinoma with relatively high frequencies and are driver genes, such as *TP53*, *SMAD4*, *ARID1A*, *PIK3CA*, *ELF3*, *CDKN2A*, *KRAS*, *ERBB2*, *ARID2*, *STK11*, *CTNNB1*, *KMT2C*, *TERT* promoter, and *RB1* [7, 8]. However, there are still few studies on GVNINs and this is partly because of the ill-established classification system for GVNINs [9].

Moreover, the relationship between these GVNIN cases and PGA remains unknown. Some otherwise typical ICPN cases, partly contain MUC6-positive or PGA-like lesions, and hence, the possibility that PGA may progress to ICPN remains unproven. Some PGA or ICTN-like cases contain both mucinous and non-mucinous epithelia; hence, the possibility that PGA may progress to ICTN, or vice versa, remains unclear.

Hence, this study aimed to establish a relevant clinicopathologic classification system for GVNINs and to determine the relationship between PGA and other group tumors in terms of tumorigenesis. We collected all types of GVNINs and classified them by gross and histological appearance as well as histological subtypes (differentiation direction), and analyzed their clinicopathologic, immunohistochemical, and molecular features. We used immunohistochemistry (IHC) which has been reported to be a surrogate marker of molecular abnormalities of recently reported gallbladder carcinoma [7, 8]. Additionally, we focused on the tumorigenesis of GVNINs containing MUC6-positive, PGA-like lesions.

Materials and methods

The institutional review board at Juntendo University approved this study (approval codes: #M17-0099).

Materials

In total, 85 cases with GVNINs of the gallbladder were included in this study. Of the 148 surgically resected and pathologically confirmed cases of gallbladder adenoma or carcinoma in Juntendo University hospital between January 2004 and January 2024, 79 surgical cases were extracted which contained elevated (> 5 mm from the neighboring mucosa [10]) gallbladder tumors (inclusion criterion), did not receive preoperative chemotherapy (exclusion criterion), and had pathologic diagnoses other than adenocarcinoma, such as squamous cell carcinoma and neuroendocrine carcinoma (exclusion criterion). Also, the authors received six consultations of surgical cases which satisfied the inclusion/exclusion criteria. Hence, a total of 85 GVNIN cases were included in this study. Of the 85 GVNIN cases, 15 were used in our previous study [11].

Classification of GVNIN

First, GVNINs were grossly and microscopically classified into two groups: “pedunculated group (PE)” and “sessile group (SE)”. Cases where the entire tumor was connected to the gallbladder wall with an intervening thin stalk, which was covered by non-tumorous epithelia, were classified as PE. Conversely, cases where the tumor was connected to the gallbladder wall with a broad base, and the tumor stalk was covered by tumorous epithelia, were considered SE. There were 27 cases in which the whole or part of the tumor was observed as “dropped” following post-operative procedures. Of these 27 cases, 22 were classified as “PE (dropped)” because a non-tumorous stalk component was detected among the dropped tumor and/or no tumor was detected at the tumor base of the gallbladder mucosa. Five cases were classified as “SE (dropped)” when non-tumorous stalk component was not detected in the dropped tumor and/or part of the tumorous component remained at the tumor base of the gallbladder mucosa.

In addition, SE tumors were further classified into type 1 (SE1) and type 2 (SE2). Cases with homogeneous histology harboring very thin tumor stroma/stalks were grouped as SE1, while others with heterogeneous histology, sometimes with thick and fibrous tumor stroma, were considered SE2, referring to the classification of IPNBs [12, 13].

Clinicopathologic data collection

Clinicopathologic features, including patients’ age, sex, tumor size (maximal diameter and tu-

mor height from the surrounding mucosa), and TNM stage according to the Union for International Cancer Control [14], were collected. In cases which the tumor was not invasive, we determined the case as carcinoma in situ (or pTis) when p53 overexpression with IHC, tumor necrosis, or cribriform formation was observed, and otherwise as adenoma.

Evaluation of tumor histology

All gallbladder specimens had been cut longitudinally from the gallbladder fundus to the neck, and 2-8 slices comprising of 6 to 56 glass slides were available, depending on the tumor size and gallbladder size, for histological review of this study. After reviewing all glass slides, the representative 2-3 slices (6 to 12 glass slides) were selected and used for the following data collection. Data included the ratio of tubular and papillary components, ratio of mucin-rich tumor cell among the entire tumor cells, existence of squamoid morule, and tumor replacement to the neighboring mucosa; non-elevated mucosa was evaluated with hematoxylin and eosin-stained specimen and periodic-Acid-Sciff (PAS) stained specimen.

Histological subtyping with IHC

Tumor subtype/differentiation direction was determined with the help of IHC for MUC1, MUC2, MUC5AC, MUC6, and CDX2. The results of IHC for MUCs and CDX2 were as follows: positive, when > 50% of the tumor cells were positive for these antibodies, and otherwise negative. Cases comprised of tumor cells resembling colonic villous adenoma or adenocarcinoma and positive for MUC2 and/or CDX2 were determined as intestinal type, while those comprised of roundish to cuboidal cells without evident cytoplasmic mucin and positive for MUC1 were considered pancreatobiliary type. Moreover, cases composed of tumor cells resembling gastric foveolar cells or pyloric gland cells and positive for MUC5AC and/or MUC6 were determined to be gastric type. Gastric type was further divided into gastric foveolar type (mainly comprising of MUC5AC-positive cells) and gastric pyloric type (mainly comprising of MUC6-positive cells). Cases comprised of homogeneous cuboidal cells with less cytoplasmic mucin but positive for MUC6 were also included in the gastric pyloric type.

IHC surrogating for molecular status and Ki-67

To investigate the molecular status of the tumor, IHC stains for β-catenin, SMAD4, p53, STK11, ARID1A, and HER2 were performed. To evaluate the proliferating activity, IHC for Ki-67 was performed. All IHC except SMAD4 and STK11 were performed for all study cases (n = 85), and IHC for SMAD4 and STK11 were performed for 80 cases, because of the shortage of tumor specimen after performing the other examinations in five cases in the pedunculated tumor group. Deparaffinized 4-μm sections from each paraffin block were exposed to 0.3% hydrogen peroxide for 10 min to block endogenous peroxide activity. Normal background gallbladder mucosa and breast cancer specimens were used as a positive control for β-catenin, SMAD4, p53, STK11, ARID1A and HER2, respectively. Details of the primary antibodies used in this study are summarized in **Table 1**. HER2-IHC was performed on the BenchMark®XT automated slide stainer (I-VIEV put HER2/neu kit, Ventana Medical Systems) following the manufacturer's instructions and other IHCs were performed manually. Regarding the IHC for β-catenin and Ki-67, the nuclear-positive ratio (labeling indices) was recorded. Concerning IHC for SMAD4 and ARID-1A, the existence of tumor area with nuclear loss was evaluated, while for STK11, cytoplasmic loss was evaluated. Regarding IHC for p53, the overexpression of nuclei was evaluated. Evaluation of HER2-IHC was performed according to the scoring system for gastric carcinoma, scoring 0-3 [15].

Somatic mutational analyses of KRAS, GNAS, and CTNNB1

Mutational analyses were performed for all SE group tumors (n = 29) and a part of the PE group tumors (the number of cases analyzed is shown in **Table 4**), because of the shortage of tumor DNA required for analysis due to the small tumor size for some cases with PE tumors. *CTNNB1* data for 15 of the PE group tumors were already obtained in our previous study [11]. Since there were some SE1 cases containing tubular adenoma-like or PGA-like lesions with β-catenin nuclear-accumulation, *CTNNB1* mutational analysis was performed separately for these PGA-like area and other areas to determine the relationship of PGA-like lesions and other lesions in terms of molecular abnor-

Table 1. Antibodies used in this study

Antibody	Clone	Dilution	Pretreatment*	Source
MUC1	Ma695	1:100	HIER	Leica Biosystems, New Castle, UK
MUC2	Ccp58	1:100	HIER	Leica Biosystems, New Castle, UK
MUC5AC	CLH2	1:100	HIER	Leica Biosystems, New Castle, UK
MUC6	CLH5	1:100	HIER	Leica Biosystems, New Castle, UK
CDX2	CDX2-88	1:100	HIER	Bio Genex, Fremont, USA
Ki-67	MIB-1	1:200	HIER	DAKO, Glostrup, Denmark
β-catenin	β-catenin-1	1:100	HIER	DAKO, Glostrup, Denmark
P53	1801	ready to use	HIER	Bio Genex, Fremont, CA, USA
HER2	4B5	ready to use	HIER	Ventana, Roche Tissue Diagnostics, Tucson, AZ, USA
STK11 (LKB1)	D60C5F10	1:250	HIER	Cell Signaling Technologies, Danvers, MA, USA
ARID1A	Polyclonal (HPA005456)	1:500	HIER	Sigma Aldrich, St. Louis, MO, USA
SMAD4	B-8	1:50	HIER	Santa Cruz Biotechnology, Dallas, TX, USA

*HIER; heat-induced epitope retrieval.

Table 2. Primers used in this study

Gene	Exon	Forward	Reverse
CTNNB1	3	TTTGATGGAGTTGGACATGG	CAGGACTTGGGAGGTATCCA
KRAS	2	AAGGCCTGCTGAAAATGAC	TGGTCCTGCACCAGTAATATG
KRAS	3	TGGAGAAACCTGTCTCTTGGA	ACACAAAGAAAGCCCTCCCC
GNAS	8	GTTGGCTTTGGTGAGATCCA	AGGTAACAGTTGGCTTACTGGA
GNAS	9	CTGGAATAACCAGCTGTCCTC	TCCCTAACAACACAGAAGCAAA

malities. Tumor DNA was extracted from 20-40 serial unstained sections (6 mm) of tumor specimens. The selected areas were manually dissected with sterilized disposable blades under a microscope. DNA isolation was conducted using QIAmp DNA kit (Qiagen, Hilden, Germany). The samples were analyzed and the PCR was conducted in triplicates for each sample with pairs of primers encompassing exon 2 and 3 of *KRAS*, exons 8 and 9 of *GNAS*, and exon 3 of *CTNNB1*. Information on the primers is shown in **Table 2**. The electrophoresis of the PCR products was performed in 2% Agarose gel, and recovered DNA was submitted to Eurofine Genomics, Co., Ltd., Tokyo, Japan, for sequencing. Mutations were confirmed if the height of the mutated peak reached 20% of the height of the normal peak for both sense and anti-sense directions.

Evaluation of the ratio of mucinous epithelia in PE type tumors and analysis of its significance

To evaluate the clinicopathological and molecular differences between PE type tumors composed mostly of mucinous tumor epithelia and those composed mostly of non-mucinous tumor epithelia, the percentages of mucinous epithelium and non-mucinous epithelium was recorded in 5% increments. The existence of intracytoplasmic mucin was determined with PAS-stained specimens. Moreover, the relationship of the percentages of mucinous epithelia to the clinicopathologic, histological, immunohistochemical, and molecular data was evaluated.

Statistical analysis

Comparison of categorical data among the groups was performed with Fisher' exact test and that of serial data was with Mann-Whitney's U test. Correlation between mucinous percentage and other data was evaluated using Spearman's rank correlation coefficient with GraphPad Prism® software, ver. 9.5 (GraphPad, San Diego, CA, USA).

Results

Clinicopathologic data of our GVNINs

Table 3 shows the summary of our study cohort. The mean patient age was 57, 80, and 70 years for PE, SE1, and SE2 groups, respectively. The PE group had younger individuals com-

Table 3. Clinicopathological and histological features of grossly visible non-invasive neoplasms of the gallbladder

	Pedunculated (PE) (n = 56)	Sessile (SE)		*p*¶		
		Type 1 (n = 6)	Type 2 (n = 23)	PE vs SE1	PE vs SE2	SE1 vs SE2
Clinicopathological features						
Age, mean (year) (range)	57 (32-87)	80 (76-83)	70 (42-85)	****	****	**
Sex, Male/Female	31/25	2/4	13/10	*NS*	*NS*	*NS*
Tumor						
Size, mean (mm) (range)	12.8 (5-37)	31.8 (14-50)	63.1 (14-200)	***	****	*
Height, mean (mm) (range)	8.1 (5-22)	13.2 (5-25)	8.5 (5-24)	*NS*	*NS*	*NS*
≤ Tis/T1a or T1b/T2 ≤ (%)	56 (100)/0 (0)/0 (0)	4 (66.7)/1 (16.7)/1 (16.7)	2 (8.7)/3 (13.0)/18 (78.2)	**	****	**
Histological features						
Tub ratio, mean (%) (range)φ	92.0 (75-100)	54.2 (5-85)	22.4 (0-75)	***	****	*
Muc ratio, mean (%) (range)φ	40.0 (0-100)	64.2 (10-100)	32.4 (5-75)	*NS*	*NS*	*
Sq. morule, present (%)φ	24 (42.9)	0 (0)	0 (0)	*NS*	****	*NS*
Lat. spread, present (%)φ	0 (0)	4 (66.7)	21 (91.3)	****	****	*NS*
Subtype						
Gf/Gp/Gf+Gp/ PB/INT/Mix (%)§	0 (0)/56 (0)/0 (0)/ 0 (0)/0 (0)/0 (0)	1 (16.7)/3 (50.0)/2 (33.3)/ 0 (0)/0 (0)/0 (0)	1 (4.3)/0 (0)/1 (4.3)/ 8 (34.8)/5 (21.7)/8 (34.8)	*NS*	****	****

φTub ratio, the ratio of tubular growth (%), Muc ratio, the ratio of mucinous tumor cells, Sq. morule, squamoid morule, and Lat. Spread, tumor replacing lateral neighborhood epithelia. §Gf, gastric foveolar type, Gp, gastric pyloric type, PB, pancreatobiliary type, INT, intestinal type, and MIX, more than two types, mixed. ¶For subtype, p value was obtained for the ratio of gastric subtypes among all subtypes. ****, < 0.0001, ***, < 0.001, **, < 0.01, *, < 0.05.

pared to SE1 and SE2 groups ($P < 0.0001$ for both), and SE2 had younger individuals compared to the SE1 group ($P = 0.0059$). Female percent was 44.6%, 66.7%, and 43.5%, for PE, SE1, and SE2 groups, respectively, and there was no significant difference between the groups. Mean tumor size/height was 12.8 mm/8.1 mm, 31.8 mm/13.2 mm, and 63.1 mm/8.5 mm for PE, SE1, and SE2 groups, respectively. PE group had cases with smaller tumor size than those in the SE1 and SE2 groups ($P = 0.0007$ and < 0.0001, respectively) and SE1 was smaller than SE2 ($P = 0.0152$). There was no significant difference in tumor height between the groups. There were no PE group tumors with stromal invasion (pTis or less), whereas 16.7%/16.7% of SE1 and 13.0%/78.2% of SE2 showed stage pT1/pT2 or more, respectively ($P < 0.01$, 0.0001, and 0.01 between PE and SE1, PE and SE2, and SE1 and SE2, respectively).

Histologically, a tubular pattern was more predominant in PE than in SE1 and SE2 ($P = 0.0004$ and < 0.0001, respectively) and in SE1 than SE2 ($P < 0.05$). Mucin-containing cells were more in SE1 than in SE2 ($P < 0.05$). Regarding histological subtyping, all PE tumors belonged to gastric pyloric type (Gp); all SE1 tumors belonged to gastric foveolar (Gf), and Gp or mixed Gf+Gp type (16.7%, 50.0%, 33.3%, respectively). Conversely, PB type (34.8%) and intestinal type (INT) (21.7%) were more frequent than gastric (G) type (8.6%) in SE2 tumors.

IHC surrogating for molecular status and Ki-67 of GVNINs

IHC results are summarized in **Table 4** and representative microscopic view and IHC results are shown in **Figures 1**-**3**. Briefly, β-catenin nuclear accumulation was observed in 100%, 66.7%, and 30.4% of PE, SE1, and SE2 tumors, respectively. STK11-loss was observed in 0%, 83.3%, and 17.4% of PE, SE1, and SE2 tumors, respectively. All SE1 tumors with β-catenin nuclear accumulation showed both STK11-loss and *CTNNB1* mutation. All SE2 tumors, except one, with β-catenin nuclear accumulation did not show CTNNB1 mutation nor STK11-loss (**Table 4**).

SMAD4-loss was detected exclusively for the intestinal subtype of SE2. HER2 scores of 2/3 were observed exclusively for and 13.0%/13.0% of SE2 cases, respectively. ARID1A-loss was not observed exclusively in any of the study cases (0%). p53 overexpression was detected in 1.8%, 16.7%, and 73.9% of PE, SE1, and SE2 cases, respectively ($P = 0.186$, < 0.0001, and $= 0.019$ for PE vs. SE1, PE vs. SE2,

Table 4. Immunohistochemical and mutation data of grossly visible non-invasive neoplasm of the gallbladder

GVNIN	PE (n = 56)	SE-1 (n = 6)			SE-2 (n = 23)				
subtype[§]	Gp (n = 56)	Gf (n = 1)	Gp (n = 3)	Gf+p (n = 2)	Gf (n = 1)	Gf+p (n = 1)	PB (n = 8)	INT (n = 5)	Mix (n = 8)
IHC[φ]									
β-catenin, nuclear	56 (100)	0 (0)	3 (100)	1 (50)	0 (0)	1 (100)	3 (37.5)	0 (0)	3 (37.5)
STK11-loss	0 (0)	0 (0)	3 (100)	2 (100)	0 (0)	1 (100)	0 (0)	0 (0)	3 (37.5)
SMAD4-loss	0 (0)	0 (0)	0 (0)	0 (0)	0 (0)	0 (0)	0 (0)	3 (60.0)	0 (0)
HER2-score 2	0 (0)	0 (0)	0 (0)	0 (0)	1 (100)	0 (0)	0 (0)	1 (20.0)	1 (7.5)
HER2-score 3	0 (0)	0 (0)	0 (0)	0 (0)	0 (0)	0 (0)	2 (15.0)	0 (0)	1 (7.5)
ARID1A	0 (0)	0 (0)	0 (0)	0 (0)	0 (0)	0 (0)	0 (0)	0 (0)	0 (0)
p53-o.e.	1 (1.8)	0 (0)	1 (33.3)	0 (0)	1 (100)	1 (100)	5 (62.5)	4 (80.0)	6 (75.0)
Ki-67 LI	14 (1-55)	40 (40)	11 (4-16)	7 (6-8)	30 (30)	35 (35)	38 (28-50)	51 (40-75)	32 (4-83)
Mutation[φφ]									
CTNNB1 ex3	41/41 (100)	0/1 (0)	3/3 (100)	2/2 (100)	0/1 (0)	0/1 (0)	0/8 (0)	0/5 (0)	1/8 (12.5)
KRAS ex2	4/41 (7.1)	0/1 (0)	1/3 (33.3)	0/2 (0)	0/1 (0)	0/1 (0)	1/8 (12.5)	0/5 (0)	0/8 (0)
KRAS ex3	0/41 (0)	0/1 (0)	0/3 (0)	0/2 (0)	0/1 (0)	0/1 (0)	0/8 (0)	0/5 (0)	0/8 (0)
GNAS ex8	0/10 (0)	0/1 (0)	0/3 (0)	0/2 (0)	0/1 (0)	0/1 (0)	0/8 (0)	0/5 (0)	0/8 (0)
GNAS ex9	0/10 (0)	0/1 (0)	0/3 (0)	0/2 (0)	0/1 (0)	0/1 (0)	0/8 (0)	0/5 (0)	0/8 (0)

[§]Histological subtype; Gp, gastric pyloric type; Gf, gastric foveolar type; PB, pancreaobiliary type, I, intestinal type, Mix, more than two types, mixed. [φ]IHC, immunohistochemistry; number of cases with b-catenin nuclear accumulation, STK11-loss, and p53-o.e. (overexpression) are shown with their percentages in parenthesis. Ki-67 LI, labeling index is shown in % and its range is in parenthesis. [φφ]Mutation, number of cases with point mutation of each gene was shown with their percentages in parenthesis.

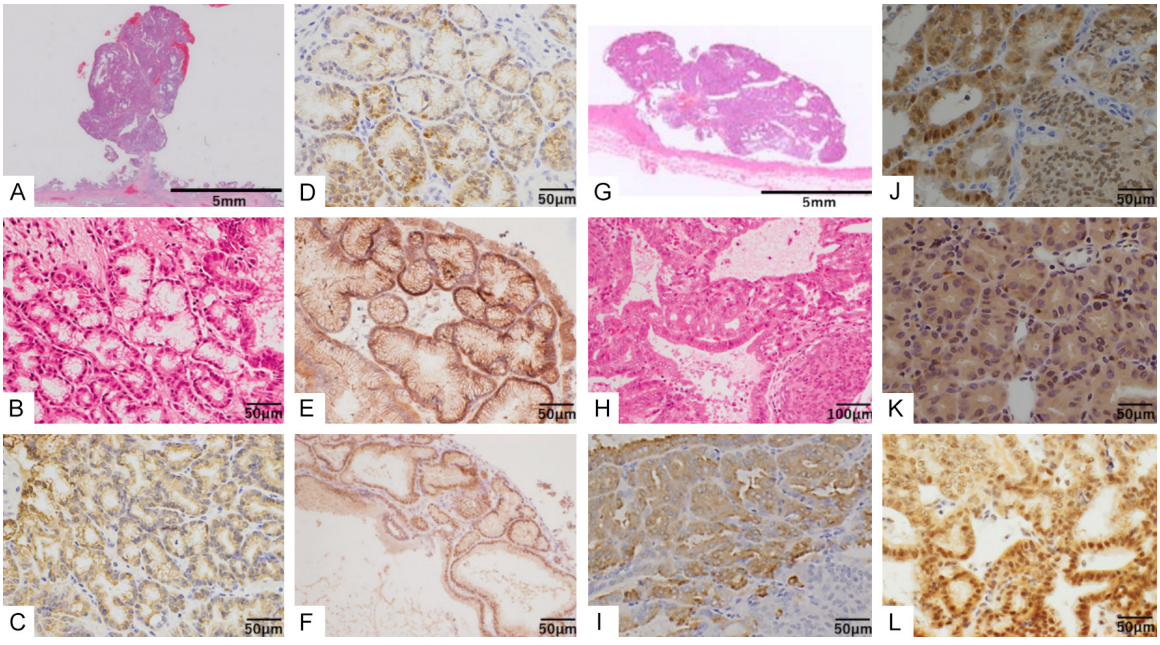

Figure 1. Grossly visible noninvasive neoplasm of the gallbladder (GVNIN), pedunculated (PE) group. (A-F) PE group, mucinous cell-dominant, (G-L) PE group, nonmucinous cell-predominant. Both cases showed tubular growth (B, H) and were diffusely positive for MUC6 (C, I). Both showed nuclear accumulation of β-catenin (D, J), STK11-non-loss (E, K), and SMAD4-non-loss (F, L). Bar = 5 mm (A, G), 50 mm (B-F, I-L), 100 mm (H). H&E [A, B, G, H].

and SE1 vs. SE2, respectively). The mean value of the Ki-67 labeling index was 14.1%, 14.5%, and 37.9% for PE, SE1, and SE2, respectively and it was significantly higher in SE2 compared to PE and SE1 ($P < 0.0001$ and < 0.0051, respectively).

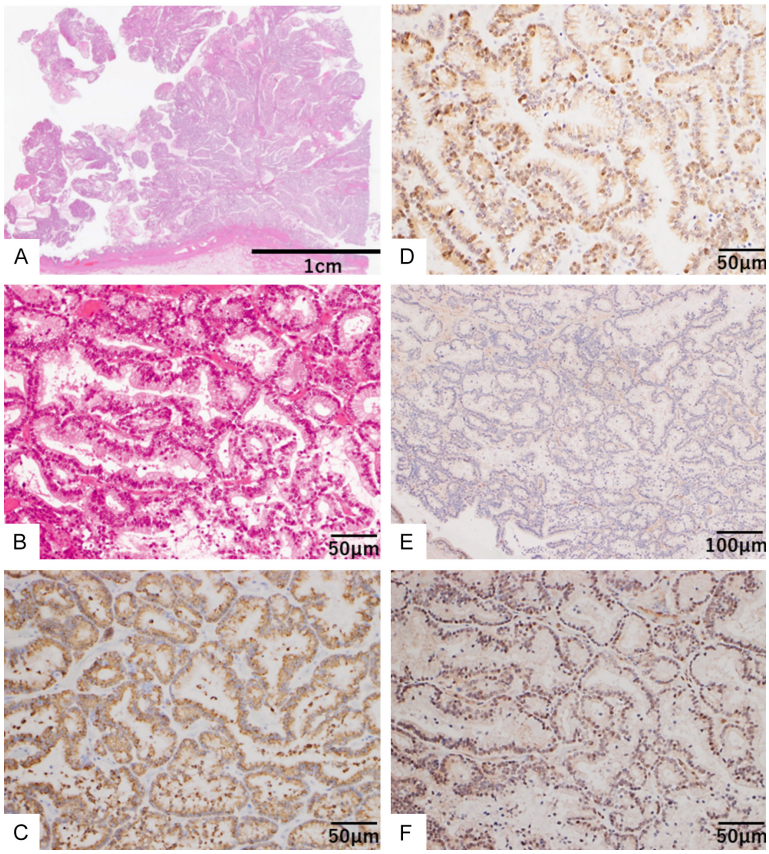

Figure 2. Grossly visible noninvasive neoplasm pf the gallbladder (GVNIN), sessile type1 (SE1) [gastric foveolar and pyloric type]. Some tumor areas showed similar histology to pyloric gland adenoma (B), diffusely positive for MUC6 (C), and showed nuclear accumulation of β-catenin (D), Tumor area had STK11-loss, and background gallbladder mucosa did not have STK11 loss (E), and did not have SMAD4 loss (F). Bar = 1 cm (A), 50 mm (B-D, F), 100 mm (E).

Somatic mutational analyses of KRAS, GNAS, and CTNNB1

The frequency of missense mutation of *KRAS* (exon 2 and 3), *GNAS* (exon 8 and 9), and *CTNNB1* (exon 2) for each tumor group is summarized in **Table 4**. Summarily, *CTNNB1* mutation was detected in 100%, 83.3%, and 4.3% of PE, SE1, and SE2 tumors, respectively (P = 0.128 for PE vs. SE1, < 0.0001 for PE vs. SE2, and = 0.0003 for SE1 vs. SE2, respectively). We performed mutational analyses separately for PGA-like area and other areas in five of SE type 1 cases, which showed PGA-like areas and other areas of these cases harbored a common *CTNNB1* mutation in all five cases (**Figure 4**).

Missense mutation of *KRAS* was detected in 9.8% (including 4.9% of cases with variant of uncertain significance, according to cBioPortal for Cancer Genomics; https://www.cbioportal.org), 16.7%, and 4.3% of PE, SE1, and SE2 tumors, respectively. Missense mutation of *GNAS* exon 8 and 9 was not detected in any PE, SE1, and SE2 cases.

Evaluation of the ratio of mucinous epithelia in PE type tumors and analysis of its significance

Using PAS stain, non-mucinous tumor cells characterized by cuboidal to short columnar cells without obvious cytoplasmic mucin were present, at least focally, in all 56 (100%) PE cases. The amount of non-mucinous tumor cells ranged from 0% to 100% (**Table 5**). There was a significant relationship between the ratio of mucinous tumor cells and patients' age/β-catenin LI of the tumor (P < 0.05, < 0.0001, respectively) (**Figure 5**). The other clinicopathological features including patients' sex distribution, tumor size/height, the ratio of histological squamoid morule formation and Ki-67 LI were not different for the ratio of mucinous epithelia of the tumor.

Discussion

The present study classified gallbladder GVNINs grossly into the PE and SE groups, and further classified the SE group histologically into SE1 and SE2. The latter classification was according to the recently proposed classification system of IPNBs [12]. Clinical data of these three groups, such as tumor stage distribution, were significantly different suggesting that the present GVNIN classification is clinically relevant. Stromal invasion of the tumors was seen in 0%, 33.4%, and 91.2% of the PE, SE1, and SE2 tumors. Most SE2 tumors were stage pT2 or more, while only 16.7% of SE1 tumors were pT2 or more. The better prognosis of the PE-type tumor compared to the SE-type tumor has been

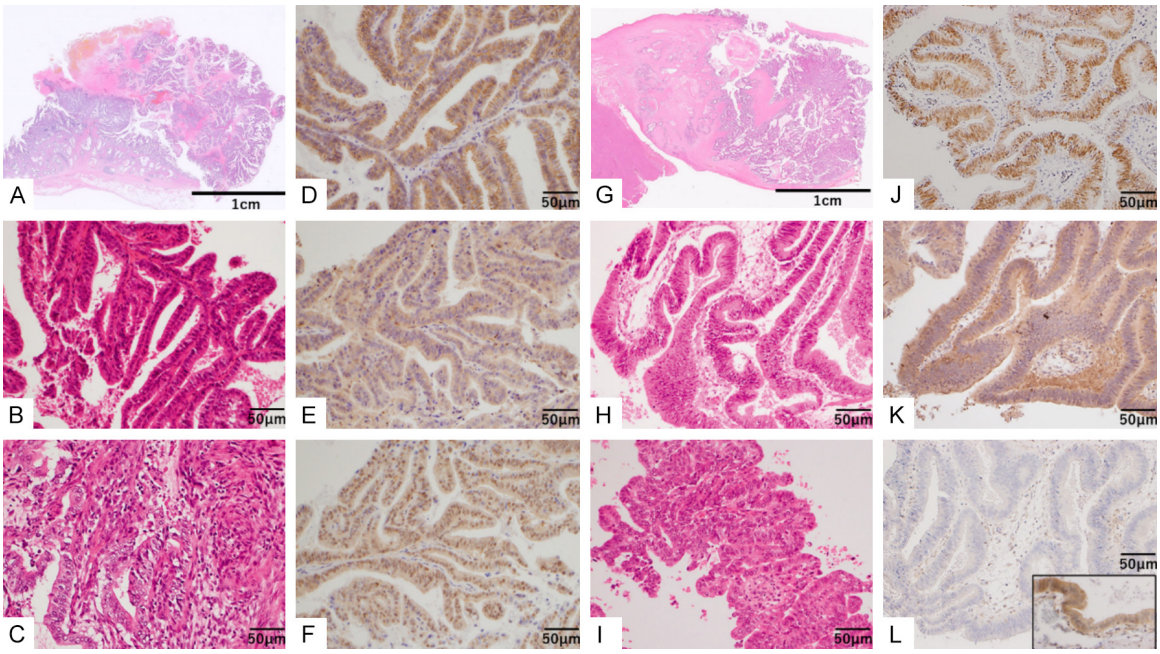

Figure 3. Grossly visible noninvasive neoplasm of the gallbladder (GVNINs), sessile type2 (SE2). (A-F) pancreatobiliary type, (G-L) intestinal type. Both showed predominantly papillary growth (B, H) and had heterogeneously thick stroma (C, I). No nuclear accumulation of β-catenin (D), non-loss of STK11 (E), and non-loss of SMAD4 (F) for the pancreatobiliary type, and CDX2-positive (J), non-loss of STK11 (K), and loss of SMAD4 for the intestinal type. Inset of (L): background gallbladder mucosa was positive for SMAD4. Bar = 1 cm (A, G), 50 mm (B-F, H-L). H&E [A-C, G-I].

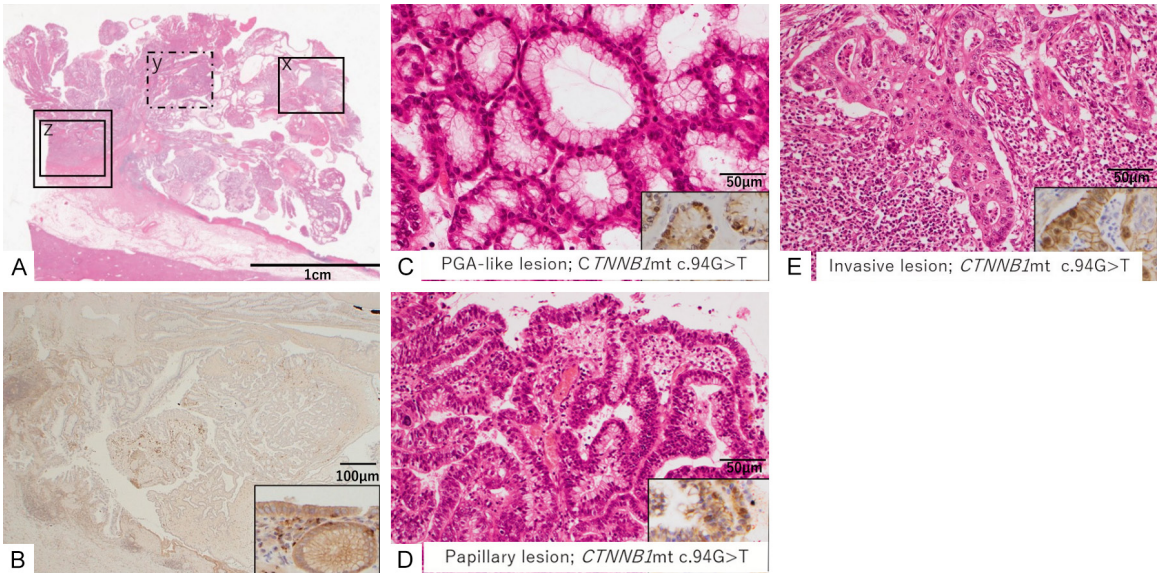

Figure 4. A representative sessile type 1 (SE1) case containing a PGA-like lesion. (A, B) Roupe view. STK11 was lost in the entire tumor (B). Inset of (B): Normal background mucosa. (C-E) Corresponds to area x (PGA-like lesion), y (non-invasive, non-PGA-like lesion), and z (invasive lesion) shown in (A). Each inset shows nuclear accumulation of β-catenin at area x-z. Bar = 1 cm (A), 100 mm (B), 50 mm (C-E). H&E [A, C-E].

already appreciated for more than 30 years [16]. Although our study had one case (1.8%) of carcinoma in situ (determined with overexpression of p53 with IHC) and no case with invasive carcinoma, Ishikawa et al., had reported that 22% (2 cases) of PE type showed stromal invasion and these two cases were larger than 30 mm, showing a higher malignant rate of PE type

Table 5. Distribution of the ratio of mucinous tumor cells in PE cases and its relationship to clinicopathological, histological, immunohistochemical, and molecular data

	Clinicopathology				Histology	Immunohistochemistry		Mutation
	Age mean (range)	Sex M/F	Size mean (range)	Height mean (range)	Sq. morule present (%)$^{\varphi}$	β-catenin$^{\varphi}$ mean (range)	Ki-67 LI$^{\varphi}$ mean (range)	*CTNNB1*$^{\varphi}$
% Mucinous$^{\varphi}$								
< 5 (n = 4)	52 (38-63)	3/1	10.8 (6-16)	7.5 (5-12)	2 (50.0)	75.0 (65-80)	10.8 (5-15)	100
5-10 (n = 16)	52 (38-71)	10/6	14.8 (8-25)	9.3 (5-22)	8 (50.0)	68.8 (30-90)	17.3 (1-70)	100
15-50 (n = 16)	61 (32-82)	8/8	12.6 (5-37)	8.1 (5-16)	8 (50.0)	45.6 (10-90)	14.1 (5-55)	100
55-85 (n = 11)	60 (43-87)	4/7	9.7 (5-18)	5.7 (5-8)	3 (27.3)	41.4 (10-60)	13.0 (3-40)	100
90-100 (n = 9)	61 (44-72)	6/3	14.4 (5-23)	9.1 (5-15)	3 (33.3)	23.1 (3-70)	11.4 (5-20)	100
p	*< 0.05	*NS*	*NS*	*NS*	*NS*	*< 0.0001	*NS*	*NS*

$^{\varphi}$% Mucinous cell, mucinous tumor cells among total tumor cells in %; Sq. morule, squamoid morule; b-catenin, b-catenin labeling index, and Ki-67, Ki-67 labeling index; CTNNB1, frequency (%) of *CTNNB1* mutation. * with statistical significance.

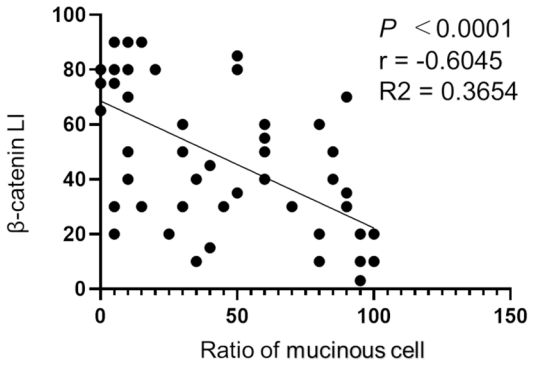

Figure 5. Relationship between the ratio of mucinous tumor cells and β-catenin labeling index (LI) in pedunculated tumors. Larger ratio of mucinous cells relates to a lower β-catenin LI ($P < 0.0001$).

tumor than that in our study. We think the discrepancy in this malignant rate may depend on the definition of PE and SE. Ishikawa et al. classified both the pedunculated type (0-Ip type in classification of the colon cancer [17]) and the semi-pedunculated type (0-Isp type) into PE, whereas we only considered 0-Ip type as PE and 0-Isp/0-Is type as SE [16].

To date, a few authors had analyzed gallbladder SE tumors by classifying them according to the recently proposed IPNB typing, as in this study. Akita et al. reported that stromal invasion rates were 57.1% and 100% for type 1 and type 2, respectively [3]. Nakanuma et al. reported the stromal invasion rates were 12.5% and 54.5% for type 1 and type 2, respectively [10]. In this study, the stromal invasion rates were 33.3% and 91.3% for SE1 and SE2. Although the invasion rate was relatively diverse depending on the study, all three studies showed a significantly more malignant nature of SE2 tumors.

The present study also showed significant differences in histological growth pattern and the distribution of histological subtypes among the three tumor groups. PE tumors were exclusively tubular and of the gastric pyloric type, SE1 were either gastric foveolar, pyloric or mixed, and SE2 were predominantly pancreatobiliary and intestinal types. With IHC, SE1 tumors were consistently positive for MUC5AC, MUC6, or both and consistently negative for MUC1, MUC2, and CDX2. In addition, SE1 tumors frequently had STK11-loss, β-catenin nuclear accumulation, and *CTNNB1* mutation. The predominance of gastric subtype and frequent STK11 gene and CTNNB1 gene abnormalities in type 1 (or SE1 in this study) tumors has been also reported in a previous study [3]. Although the sample size of both the previous study and ours were relatively small, the results of these studies together may suggest that histological differentiation towards gastric mucosa and the simultaneous occurrence of *CTNNB1* and *STK11* abnormalities are specific features of SE1 tumors. Of note, although nuclear accumulation of β-catenin and cytoplasmic STK11-loss were also observed in 26.1% of SE2 tumors, cases with β-catenin abnormalities were different from those with STK11-loss, and were *CTNNB1* mutation-free in all cases except one case. This suggests a contribution of abnormalities of the Wnt-pathway gene other than *CTNNB1* and an independent event from *STK11* abnormalities in these SE2 cases with β-catenin nuclear accumulation. *STK11* gene encodes liver kinase B1 (LKB1), a serine/threonine kinase that functions as a tumor suppressor gene. Germline mutations of *STK11* are associated with Peutz-Jeghers syndrome, an autosomal-dominant disorder. Although somatic

STK11 mutations have been reported to be uncommon except in lung and prostatic carcinoma [18], a recent study with targeted amplicon sequencing showed a relatively high rate of *STK11* mutations or STK11-loss in IPMNs [19]. Moreover, the crosstalk oncogenesis of Wnt/β-catenin signaling and STK11-loss has been reported in several tumors [20, 21].

In this study we used IHC for β-catenin, STK11, SMAD4, p53, ARID1A, and HER2 as surrogates for *CTNNB1* mutation or other Wnt pathway abnormalities, abnormalities of *STK11*, *SMAD4*, *TP53*, *ARID1A*, and amplification of *ERBB2*. The contribution of mutations of *CTNNB1* or other Wnt pathway genes to the β-catenin nuclear accumulation has been well appreciated [22]. The strong relationships of immunohistochemical loss of STK11, ARID1A, and SMAD4 with mutations of *STK11*, *ARID1A*, and *SMAD4* genes, respectively, have been reported and these IHC stains have been used as surrogate markers by several studies [19, 23-26]. Moreover, the strong relationship between HER2 overexpression and ERBB2 amplification has been reported and HER2-IHC was used as a surrogate for ERBB2 amplification by researchers [27]. A fair relationship of nuclear accumulation of p53 and *TP53* mutations has been reported [28]. Our study showed β-catenin nuclear accumulation, p53 overexpression, STK11-loss, SMAD4-loss, ARID1A-loss, and higher HER2 score (score 2-3) for 78.8%, 22.4%, 10.6%, 3.5%, 0%, and 7.1% of intraepithelial components of GVNINs, respectively. Recent next generation sequencing-derived data by Guraldo et al. reported that 6%, 63%, 6%, 19%, 18%, and 6% of gallbladder carcinoma cases harbored abnormalities of *CTNNB1*, *TP53*, *STK11*, *SMAD4*, *ARID1A*, and *ERBB2* respectively [7]. The discrepancy in our data and that of Guraldo's may be due to the inclusion of many adenoma cases and of relatively many SE1 cases in our study (for higher CTNNB1/STK11 abnormalities in this study), and the difference in the targeted area for lower frequency of p53, SMAD4, and ARID1A abnormalities in our study (intraepithelial component in this study and mostly invasive area in Guraldo's).

Although the *KRAS* and *GNAS* mutations are common events in pancreatic IPMN and IPNB [29, 30], this study showed these were rare events (*KRAS*: 3.6% for PE, 16.7% for SE1, and 4.3% for SE2; *GNAS* 0% for all tumor groups). Thus far, only a few authors have examined these genes in ICPN, but their results seem concordant with ours [3, 31].

Our study showed that some of the abnormalities of surrogate IHC were related not only to tumor groups but also histological subtypes. In addition to the relations of β-catenin nuclear accumulation/STK11-loss and gastric subtype, SMAD4-loss was exclusively observed in intestinal subtype of SE2 tumors, suggesting that there is a relationship between histological differentiation of the tumor and the abnormalities of these proteins. To our knowledge, there have been few papers reporting a relationship between histologic subtype and STK11/SMAD4 abnormalities in gallbladder tumor. According to Omori et al., STK11 abnormalities are frequent in pancreatobiliary and oncocytic type IPMN [19]. In IPNB type 1, *STK11* mutations and gastric or pancreatobiliary subtypes have been reported by Zen et al. [13]. Several studies have shown the relationship of SMAD4 abnormalities and advanced tumor stage, or in case of IPNB, SMAD4 abnormalities and type 2 IPNB [24, 29, 32].

In the present study, our PE-type GVNIN (including 22 dropped cases) were almost all (> 80%) composed of MUC6-positive tubular components and all cases harbored a *CTNNB1* mutation. All of these histological, immunohistochemical, and molecular features are common in PGA of the gallbladder [11, 33]. In our study, PE tumors contained non-mucinous tumor cells with diverse proportions and 64.3% of PE tumors were composed mainly (> 50%) of non-mucinous tumor cells. To date, it is still controversial whether these gallbladder polypoid tumors mainly composed of MUC6-positive, but non-mucinous tubular components, represent a biologically different entity from mucinous-predominant PGAs. Albores-Saavedra et al., included those adenomas mainly comprised of tumor cells with non-mucinous, eosinophilic cytoplasm in PGA [34]. Pehlivanoglu et al. have introduced a new terminology, ICTN, for these non-mucinous tumors [5]. In the present study, we have shown that most PE tumors were mixed mucinous and non-mucinous, that is, most PE tumors contained at least 5% of non-mucinous or mucinous tumor cells. Irrespective of mucinous cell ratio, these tumors were clinically low grade or noninvasive, and histologi-

cally were frequently with squamoid morule formations. With these data as well as shared *CTNNB1* mutation events may suggest these non-mucinous cell-dominant, MUC6-positive tubular adenomas are to be included in the same entity with PGAs. In this study we have also shown that the ratio of non-mucinous cells increases when the ratio of tumor cells with β-catenin nuclear accumulation increases, suggesting non-mucinous change is a progression phenomenon of PGAs.

In our study 66.7% of SE1 tumors contained PGA-like areas, that is, tumor areas composed of low-grade MUC6-positive tubular tumor cells, showing IHC-determined β-catenin nuclear accumulation, and *CTNNB1*-mutation. Thus far, the relationship between these SE1 tumors (or ICPN) and PGAs has not been examined in terms of tumorigenesis. Albores-Saavedra, et al., has shown the rare occurrence of invasive adenocarcinoma in the background of PGA [34] and more recently, Nakanuma et al. has proposed that PGA could be regarded a type of ICPN gastric type [10]. Nakanuma et al., discussed that these two tumor types shared tumor histology, such as similarity to gastric pyloric glands and well-demarcation. However, the authors also noticed the different molecular pathway of PGA and ICPN gastric type, which is β-catenin abnormalities' contribution in PGA but not in ICPN gastric type [10]. In this study all SE1 tumors containing PGA-like areas had β-catenin nuclear accumulation, STK11-loss, and *CTNNB1* mutation, although the β-catenin LIs were diverse depending on the case. Whereas all PE cases were with β-catenin nuclear accumulation, *CTNNB1* mutations, and free from STK11-loss. The different STK11-status of SE1 and PE cases in the present study, may suggest that these two tumors may be considered different tumor entities, although authors still think there remains a possibility that PGA might progress to SE1 containing PGA-like lesions by additional genetic events such as STK11. Further studies with more SE1 tumors are necessary to answer this question.

Our study has several limitations. First, although our study has shown the clinicopathological and molecular validity of separating SE1 and SE2, this study could not suggest how to differentiate these in the clinical practice. Identification of differentiating methods in presurgical stage is very much needed for personalized medicine treatment. Second, since our study did not include BilINs, it could not determine clinicopathological and molecular differences of PE, SE1, SE2 and BilINs. Finally, although our study could obtain relatively clear-cut results of β-catenin, STK11, and SMAD4 abnormalities for each histological subtype of SE tumors, it was an IHC-based study and our sample size of SE1 and SE2 were not large; hence, further studies with more samples and with molecular data are demanded.

In conclusion, a relevant clinicopathological classification system of GVNINs was proposed, in particular, when analyzing histogenesis and molecular abnormalities of GVNINs. In cases of SE tumors, the importance of histological classification was also emphasized. Moreover, our findings suggested that PGA and SE1 type containing PGA-like lesions may be different entities. Finally, PE type tumors that arenon-mucinous cell dominant and mucinous-cell dominant are suggested to be the same entity, where non-mucinous cell change might be a "progression" phenomenon in PGAs.

Acknowledgements

This work was partly supported by a Grant-in-Aid from the Japan Society for the Promotion of Sciences (JSPS) KAKENHI (Grant number #21K06912 to YF). Authors thank Dr. Yifare Maimaitiaili, and Dr. He Cong for their assistance with Sample collection and molecular analyses. We thank Ms. Shuko Nojiri, Associate Professor at the Medical Technology Innovative Center and Clinical Research and Trial Center, Juntendo University, for statistical advice. We would like to thank Editage (www.editage.jp) for English language editing.

Disclosure of conflict of interest

None.

Address correspondence to: Dr. Yuki Fukumura, Department of Human Pathology, School of Medicine, Juntendo University, 2-1-1, Juntendo Bldg. A-10F, Hongo, Bunkyo-ku, Tokyo 113-0033, Japan. Tel: +81-3-3813-3111; +81-3-3812-1056; E-mail: yfuku@juntendo.ac.jp

References

[1] Klimstra DS, Lam AK, Paradis V and Schirmacher P. Tumours of the gallbladder and extra-

hepatic bile ducts. In WHO classification of tumours of the digestive system. 5th ed. Lyon: International Agency for Research on Cancer (IARC); 2019: 265-294.
[2] Adsay V, Jang KT, Roa JC, Dursun N, Ohike N, Bagci P, Basturk O, Bandyopadhyay S, Cheng JD, Sarmiento JM, Escalona OT, Goodman M, Kong SY and Terry P. Intracholecystic papillary-tubular neoplasms (ICPN) of the gallbladder (neoplastic polyps, adenomas, and papillary neoplasms that are ≥ 1.0 cm): clinicopathologic and immunohistochemical analysis of 123 cases. Am J Surg Pathol 2012; 36: 1279-301.
[3] Akita M, Fujikura K, Ajiki T, Fukumoto T, Otani K, Hirose T, Tominaga M, Itoh T and Zen Y. Intracholecystic papillary neoplasms are distinct from papillary gallbladder cancers: a clinicopathologic and exome-sequencing study. Am J Surg Pathol 2019; 43: 783-791.
[4] Mochidome N, Koga Y, Ohishi Y, Miyazaki T, Matsuda R, Yamada Y, Aishima S, Nakamura M and Oda Y. Prognostic implications of the coexisting precursor lesion types in invasive gallbladder cancer. Hum Pathol 2021; 114: 44-53.
[5] Pehlivanoglu B, Balci S, Basturk O, Bagci P, Erbarut Seven I, Memis B, Dursun N, Jang KT, Saka B, Ohike N, Tajiri T, Roa JC, Sarmiento JM, Reid MD and Adsay V. Intracholecystic tubular non-mucinous neoplasm (ICTN) of the gallbladder: a clinicopathologically distinct, invasion-resistant entity. Virchows Arch 2021; 478: 435-447.
[6] Adsay NV and Basturk O. Dysplasia and early carcinoma of the gallbladder and bile ducts: terminology, classification, and significance. Gastroenterol Clin North Am 2024; 53: 85-108.
[7] Giraldo NA, Drill E, Satravada BA, Dika IE, Brannon AR, Dermawan J, Mohanty A, Ozcan K, Chakravarty D, Benayed R, Vakiani E, Abou-Alfa GK, Kundra R, Schultz N, Li BT, Berger MF, Harding JJ, Ladanyi M, O'Reilly EM, Jarnagin W, Vanderbilt C, Basturk O and Arcila ME. Comprehensive molecular characterization of gallbladder carcinoma and potential targets for intervention. Clin Cancer Res 2022; 28: 5359-5367.
[8] Wardell CP, Fujita M, Yamada T, Simbolo M, Fassan M, Karlic R, Polak P, Kim J, Hatanaka Y, Maejima K, Lawlor RT, Nakanishi Y, Mitsuhashi T, Fujimoto A, Furuta M, Ruzzenente A, Conci S, Oosawa A, Sasaki-Oku A, Nakano K, Tanaka H, Yamamoto Y, Michiaki K, Kawakami Y, Aikata H, Ueno M, Hayami S, Gotoh K, Ariizumi SI, Yamamoto M, Yamaue H, Chayama K, Miyano S, Getz G, Scarpa A, Hirano S, Nakamura T and Nakagawa H. Genomic characterization of biliary tract cancers identifies driver genes and predisposing mutations. J Hepatol 2018; 68: 959-969.
[9] Chung T, Oh S, Won J, Park J, Yoo JE, Hwang HK, Choi GH, Kang CM, Han DH, Kim S and Park YN. Genomic and transcriptomic signatures of sequential carcinogenesis from papillary neoplasm to biliary tract cancer. J Hepatol 2025; [Epub ahead of print].
[10] Nakanuma Y, Nomura Y, Watanabe H, Terada T, Sato Y, Kakuda Y, Sugino T, Ohnishi Y and Okamura Y. Pathological characterization of intracholecystic papillary neoplasm: a recently proposed preinvasive neoplasm of gallbladder. Ann Diagn Pathol 2021; 52: 151723.
[11] He C, Fukumura Y, Toriyama A, Ogura K, Sasahara N, Mitani K and Yao T. Pyloric gland adenoma (PGA) of the gallbladder: a unique and distinct tumor from PGAs of the stomach, duodenum, and pancreas. Am J Surg Pathol 2018; 42: 1237-1245.
[12] Nakanuma Y, Basturk O, Esposito I, Klimstra DS, Komuta M and Zen Y. Intraductal papillary neoplasm of the bile ducts. In: World Health Organization Classification of Digestive System Tumours. Lyon: International Agency for Research on Cancer; 2019: 279-282.
[13] Zen Y and Akita M. Neoplastic progression in intraductal papillary neoplasm of the bile duct. Arch Pathol Lab Med 2024; 148: 989-996.
[14] UICC TNM Classification of Malignant Tumours. 8th ed. Oxford: United Kingdom Wiley Blackwell; 2017.
[15] Hofmann M, Stoss O, Shi D, Büttner R, van de Vijver M, Kim W, Ochiai A, Rüschoff J and Henkel T. Assessment of a HER2 scoring system for gastric cancer: results from a validation study. Histopathology 2008; 52: 797-805.
[16] Ishikawa O, Ohhigashi H, Imaoka S, Nakaizumi A, Kitamura T, Sasaki Y, Shibata T, Wada A and Iwanaga T. The difference in malignancy between pedunculated and sessile polypoid lesions of the gallbladder. Am J Gastroenterol 1989; 84: 1386-90.
[17] Japanese Society for Cancer of the Colon and Rectum. Japanese Classification of Colorectal, Appendiceal, and Anal Carcinoma, 9th ed. Kanehara-shuppan, 2018.
[18] Sanchez-Cespedes M. A role for LKB1 gene in human cancer beyond the Peutz-Jeghers syndrome. Oncogene 2007; 26: 7825-7832.
[19] Omori Y, Ono Y, Morikawa T, Motoi F, Higuchi R, Yamamoto M, Hayakawa Y, Karasaki H, Mizukami Y, Unno M and Furukawa T. Serine/Threonine Kinase 11 plays a canonical role in malignant progression of KRAS -mutant and GNAS -wild-type intraductal papillary mucinous neoplasms of the pancreas. Ann Surg 2023; 277: e384-e395.

[20] Liu W, Monahan KB, Pfefferle AD, Shimamura T, Sorrentino J, Chan KT, Roadcap DW, Ollila DW, Thomas NE, Castrillon DH, Miller CR, Perou CM, Wong KK, Bear JE and Sharpless NE. LKB1/STK11 inactivation leads to expansion of a prometastatic tumor subpopulation in melanoma. Cancer Cell 2012; 21: 751-64.

[21] Wang J, Zhang K, Wang J, Wu X, Liu X, Li B, Zhu Y, Yu Y, Cheng Q, Hu Z, Guo C, Hu S, Mu B, Tsai CH, Li J, Smith L, Yang L, Liu Q, Chu P, Chang V, Zhang B, Wu M, Jiang X and Yen Y. Underexpression of LKB1 tumor suppressor is associated with enhanced Wnt signaling and malignant characteristics of human intrahepatic cholangiocarcinoma. Oncotarget 2015; 6: 18905-18920.

[22] Machin P, Catasus L, Pons C, Muñoz J, Matias-Guiu X and Prat J. CTNNB1 mutations and beta-catenin expression in endometrial carcinomas. Hum Pathol 2002; 33: 206-212.

[23] Sato N, Rosty C, Jansen M, Fukushima N, Ueki T, Yeo CJ, Cameron JL, Iacobuzio-Donahue CA, Hruban RH and Goggins M. STK11/LKB1 Peutz-Jeghers gene inactivation in intraductal papillary-mucinous neoplasms of the pancreas. Am J Pathol 2001; 159: 2017-22.

[24] Bauer AH, Basta DW, Hornick JL and Dong F. Loss of function SMAD4 nonstop mutations in human cancer. Histopathology 2023; 82: 1098-1104.

[25] Khalique S, Naidoo K, Attygalle AD, Kriplani D, Daley F, Lowe A, Campbell J, Jones T, Hubank M, Fenwick K, Matthews N, Rust AG, Lord CJ, Banerjee S and Natrajan R. Optimised ARID1A immunohistochemistry is an accurate predictor of ARID1A mutational status in gynaecological cancers. J Pathol Clin Res 2018; 4: 154-166.

[26] Sasaki M, Nitta T, Sato Y and Nakanuma Y. Loss of ARID1A expression presents a novel pathway of carcinogenesis in biliary carcinomas. Am J Clin Pathol 2016; 145: 815-825.

[27] Hiraoka N, Nitta H, Ohba A, Yoshida H, Morizane C, Okusaka T, Nara S, Esaki M, Kishi Y and Shimada K. Details of human epidermal growth factor receptor 2 status in 454 cases of biliary tract cancer. Hum Pathol 2020; 105: 9-19.

[28] Calistri D, Barzanti F, Dal Susino M, Fedriga R, Saragoni L, Bernardi L, Ricotti L and Zoli W. Correlation between p53 gene mutations and p53 protein accumulation evaluated by different methodologies. J Biol Regul Homeost Agents 2000; 14: 120-127.

[29] Aoki Y, Mizuma M, Hata T, Aoki T, Omori Y, Ono Y, Mizukami Y, Unno M and Furukawa T. Intraductal papillary neoplasms of the bile duct consist of two distinct types specifically associated with clinicopathological features and molecular phenotypes. J Pathol 2020; 251: 38-48.

[30] Furukawa T, Kuboki Y, Tanji E, Yoshida S, Hatori T, Yamamoto M, Shibata N, Shimizu K, Kamatani N and Shiratori K. Whole-exome sequencing uncovers frequent GNAS mutations in intraductal papillary mucinous neoplasms of the pancreas. Sci Rep 2011; 1: 161.

[31] Iwasaki T, Otsuka Y, Miyata Y, Einama T, Tsujimoto H, Ueno H, Ogata S and Kishi Y. Intracholecystic papillary neoplasm arising in a patient with pancreaticobiliary maljunction: a case report. World J Surg Oncol 2020; 18: 292.

[32] Takahashi K, Takeda Y, Ono Y, Isomoto H and Mizukami Y. Current status of molecular diagnostic approaches using liquid biopsy. J Gastroenterol 2023; 58: 834-847.

[33] Yanagisawa N, Mikami T, Saegusa M and Okayasu I. More frequent beta-catenin exon 3 mutations in gallbladder adenomas than in carcinomas indicate different lineages. Cancer Res 2001; 61: 19-22.

[34] Albores-Saavedra J, Chablé-Montero F, González-Romo MA, Ramírez Jaramillo M and Henson DE. Adenomas of the gallbladder. Morphologic features, expression of gastric and intestinal mucins, and incidence of high-grade dysplasia/carcinoma in situ and invasive carcinoma. Hum Pathol 2012; 43: 1506-1513.